

Spectroscopy of Technological Defects in Si Solar Cells by Analysis of Temperature Dependent Generation Currents

Jevgenij PAVLOV*, Dariusz BAJARŪNAS, Tomas ČEPONIS, Eugenijus GAUBAS, Dovilė MEŠKAUSKAITĖ

Institute of Applied Research, Vilnius University, Saulėtekio av. 9-III, LT-10222 Vilnius, Lithuania

crossref <http://dx.doi.org/10.5755/j01.ms.20.3.5194>

Received 02 August 2013; accepted 13 December 2013

The efficiency of solar cells considerably depends on the technological defects introduced by the formation of junctions, passivation layers and electrodes. Identification of these defects present in the high conductivity base layer of modern solar cells by usage of the standard techniques, such as capacitance deep level spectroscopy, is restricted by extremely small size of samples with inherent enhanced leakage current on sample boundaries. Therefore, it is important to develop the alternative methods for the defect spectroscopy in the high conductivity junction structures, to directly control a relative low concentration of the technological defects. In this work, the spectroscopy of deep traps has been performed by combining the temperature scans of the thermal generation currents extracted from barrier capacitance charging transients and capacitance deep level transient spectroscopy techniques. The dominant carrier traps ascribed to the Cu and Ni impurities were revealed.

Keywords: barrier capacitance charging current, Si, solar cell, DLTS.

1. INTRODUCTION

The efficiency of solar cell significantly depends on the technological defects introduced during the formation of junctions, passivation layers and electrodes [1]. These defects as usually act as carrier trapping centres in the bulk and at surface of solar cells. The alternative solar cell production technologies, using copper electrodes, are attractive, in order to cheapen the commercial fabrication of solar cells. However, the problem of copper diffusion into the base region appears, where metallic impurities are fast carrier traps and can make meta-stable complexes with dopants [2, 3]. This problem can partially be solved by forming the diffusion barrier, which prevents copper indiffusion [4–6]. The formation of copper electrodes on a solar cell is additionally complicated by the necessity to combine a deposition of several metals. These technological procedures should be precisely controlled to avoid a contamination of the active device layers by carrier capture and generation centres.

The high conductivity Si material base layers are commonly used in production of the modern solar cells. The problem of the usage of the standard techniques and instrumentation (such as the capacitance deep level transient spectroscopy [7, 8], C-DLTS) then appears in precise control of the introduced defects. The high conductivity base region leads to a large barrier capacitance of a junction. This requires the extremely small area samples for the application of the standard C-DLTS instruments. Consequently, the enhanced leakage current on sample boundaries is inevitable for the small area samples. Therefore, it is important to develop the alternative methods for the defect spectroscopy in the high

conductivity junction structures, to directly control a relative low concentration of metallic impurities.

In this work, the spectroscopy of the technological defects has been implemented by combining the temperature scans of the thermal generation currents extracted from barrier capacitance charging transients and the capacitance deep level transient spectroscopy (C-DLTS) techniques. Combining of these techniques enhances reliability and methodical potential in separation of the dominant carrier traps: the standard C-DLTS instruments can be applied for a limited range of device capacitance (<3 nF) and leakage currents, which unacceptably increases for small samples, necessary for usage of the standard DLT spectrometers, while a technique of the barrier capacitance charging transients allows separating of current components in time ascribed to the barrier charging and generation currents. Signals of the barrier capacitance charging even increase beneficially when enhanced area samples are employed.

2. SAMPLES AND MEASUREMENT TECHNIQUES

The tentative industry solar cells made employing of the copper technology were examined. A solar cell contains the 180 μm thick p-Si base boron doped region. The n^+ -p junction with an emitter thickness of 0.3 μm was formed by phosphor diffusion. The texturized anti-reflection and the 150 nm thick Si_3N_4 surface passivation layers were formed. The silicide layers of Ni_2Si of thickness of 0.1 μm were also deposited. The electrodes were formed depositing by chemical means the Ni and Cu layers of 250 nm and 20 μm thickness, respectively.

The solar cell fragments of $(4 \times 4) \text{mm}^2$ were cut for the C-DLTS measurements, as the commercial DLTS instruments enable compensation of the steady-state barrier

*Corresponding author. Tel.: +370-5-236-6082, fax: +370-5-236-6003.
E-mail address: jevgenij.pavlov@tmi.vu.lt (J. Pavlov)

capacitance of values less than 3 nF. It has been found within the DLTS measurements that the nickel-copper electrodes are insufficiently proof for the temperature cycling in the range of 50 K–300 K. Therefore, several samples were made using the 100 nm thick gold electrodes deposited by a magnetron sputtering, after the copper electrode had been removed.

The C-DLTS measurements have been implemented by using a HERA-DLTS System 1030 spectrometer. The sample is connected to electrodes on sample holder within a closed-cycle He cryostat. The barrier capacitance changes (due to carrier traps) are directly recorded as the capacitance transients by using a Boonton capacitance meter installed within the HERA-DLTS System 1030 spectrometer. The capacitance transient signals are transferred to the base unit of the spectrometer, which is equipped with a voltage source, a low-pass filter and an amplifier. The C-DLTS measurement procedures are controlled by a personal computer with installed Phys-Tech software. This Phys-Tech software also contains a trap identification library using the extracted trap signatures such as the carrier capture cross-section and trap thermal activation energy. The appropriate C-DLTS regime is initially determined by setting the reverse bias voltage and the electrical injection pulse duration and amplitude. To avoid the copper electrode damage caused by temperature cycling, the frequency scans at fixed temperatures have been made for the primary defect identification.

The barrier evaluation by using linearly increasing voltage (BELIV) technique [9–11] has also been applied for the more comprehensive characterization of the solar cells. The BELIV technique for reverse biased junction is based on the analysis of barrier capacitance (C_b) changes with linearly increasing voltage $U = At$ pulse. The C_b dependence on voltage and thereby on time t can be described in depletion approximation [7]. This approximation leads to a relation $C_b = C_{b0}(1 + U/U_{bi})^{-1/2}$ for the abrupt junction, where barrier capacitance for non-biased diode of area S is $C_{b0} = \varepsilon\varepsilon_0 S/w_0 = (\varepsilon\varepsilon_0 S^2 eN_D/2U_{bi})^{1/2}$. The other symbols represent: ε_0 is the vacuum dielectric constant, ε is the material permittivity, e is the elementary charge, U_{bi} is the built-in potential barrier, $w_0 = (2\varepsilon\varepsilon_0 U_{bi}/eN_D)^{1/2}$ is a width of depletion for non-biased junction, $A = U_p/\tau_{PL}$ is the ramp of LIV pulse of the U_p amplitude and of τ_{PL} duration. The time dependent changes of charge $q = C_b U$ within junction determine a current transient $i_C(t)$:

$$i_C(t) = \frac{\partial U}{\partial t} \left(C_b + U \frac{\partial C_b}{\partial U} \right) = AC_{b0} \frac{1 + \frac{At}{2U_{bi}}}{\left(1 + \frac{At}{U_{bi}}\right)^{3/2}}. \quad (1)$$

This transient contains an initial ($t = 0$) step AC_{b0} due to displacement current and a descending constituent governed by charge extraction. In materials containing considerable density of deep traps, the generation current component appears. This current $i_g(t) = en_i w_0 (1 + At/U_{bi})^{1/2} / \tau_g$ increases with voltage $U(t)$ and can exceed the barrier charging current in the ulterior range of pulsed transient when carrier generation lifetime τ_g is rather short. Then transient of the total reverse current is described by a sum of the ($i(t) = i_C(t) + i_g(t)$) currents:

$$i(t) = AC_{b0} \frac{1 + \frac{At}{2U_{bi}}}{\left(1 + \frac{At}{U_{bi}}\right)^{3/2}} + \frac{en_i S w_0}{\tau_g} \left(1 + \frac{At}{U_{bi}}\right)^{1/2}. \quad (2)$$

The descending charge extraction and ascending generation current variation with LIV pulse time (voltage) implies existence of a current minimum within a transient. The carrier generation lifetime τ_g can be evaluated by using Eq. (2). Variations of the generation current with temperature are employed for the extraction of values of the temperature dependent generation lifetime. The latter characteristic contains the main carrier trap signatures, as the carrier capture cross-section, trap activation energy and density. The range of the inherent generation lifetimes can be examined by changing linearly increasing voltage pulse duration, and it has been varied in the range of 1 μ s–100 ms, in these experiments.

The BELIV current transients are registered using a 50 Ω load and a closed input of the Agilent Technologies DSO-X 3032A oscilloscope. Additionally, the measurement circuitry contains an adjusted output of a generator of linearly increasing voltage (LIV) and a device under investigation, connected in series. The sample is installed on a cold finger of the liquid nitrogen cryostat, for the temperature scans of the generation current transient.

3. RESULTS AND DISCUSSION

The C-DLTS measurements have been implemented by varying a rate window at fixed temperature. This regime is preferential to exclude the capture cross-section variations with temperature. The temperature dependent changes of the DLT spectrum are presented in Fig. 1. Here, the majority carrier trap ascribed peaks (i. e. hole in p-type Si base region) appear within DLT spectrum.

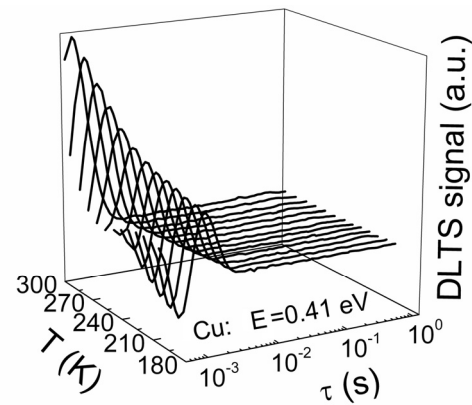


Fig. 1. The C-DLTS scans in the as-fabricated Si solar cell with Ni-Cu electrodes at different temperatures

It can be noticed in Fig. 1 the formation of two DL peaks in the range of lower temperature wing of $T \leq 240$ K, while a single deep level peak dominates in the range of elevated temperatures, $T > 240$ K. Using the pairs (T_{peak}, τ) of the peak temperature and the emission lifetime parameters, the Arrhenius graph is as usual plotted. The activation energy E of the majority carrier trap in p-Si $E_{\text{Cu-1}} = (0.41 \pm 0.01)$ eV has then been extracted from the Arrhenius plot. Additionally, a peak with

$E_{Cu-2} = (0.22 \pm 0.01)$ eV is implied. These DLTS signatures ($E_{Cu-1} = (0.41 \pm 0.01)$ eV, $T_{peak} \sim 242$ K and $E_{Cu-2} = (0.22 \pm 0.01)$ eV, $T_{peak} \sim 120$ K) with capture cross-section $\sigma \sim 5 \times 10^{-13}$ cm² are inherent for the Cu ascribed traps in Si [1, 12], where values of $E_{Cu-1} = 0.40$ eV and $E_{Cu-2} = 0.24$ eV are presented, respectively. The activation energy of $E_{Ni} \sim 0.21$ eV–0.23 eV, attributed to the Ni impurities in Si, is also referenced in literature [1, 12], although with the less value (of $\sigma \sim 10^{-16}$ cm² [12]) of the carrier capture cross-section.

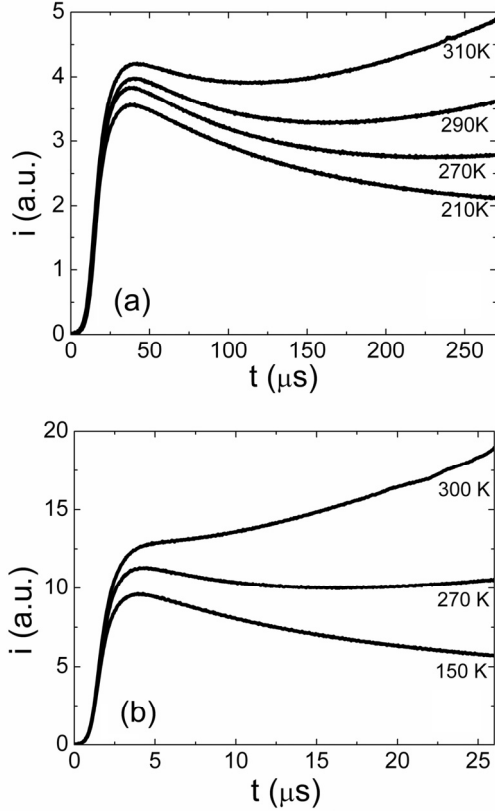


Fig. 2. Barrier capacitance (BELIV) transients recorded at different temperatures on Si solar cell fragments with Ni/Cu (a) and Au (b) top-electrodes

To clarify the impact of the Ni/Cu electrode thermal instability and to exclude the leakage current enhancement (inherent for the small area junction structures), the BELIV temperature scans were performed on the bigger fragments of the industrial solar cell using the Ni/Cu and Au top-electrodes. In Fig. 2, the temperature dependent changes of the BELIV transients are illustrated for both the Ni/Cu (a) and Au (b) top-electrodes.

It can be noticed in Fig. 2 that the resolvable generation current increase within the recorded BELIV transients is obtained for temperatures above 270 K. Also, the current is larger for the gold top-electrode containing samples. While, the generation current can reliably be resolved for the longer LIV pulse duration in Ni/Cu electrode containing solar-cell fragments. However, the measurements using Ni/Cu electrode can be performed only a few times, due to the destroyed adhesion of the metal layer. As discussed in presentation of the BELIV method principles, the generation current is added to the barrier capacitance charging/charge extraction current

component in BELIV transients. Therefore, the sum of the currents increases with enhancement of the thermal emission from traps. On the other hand, the increase of the LIV pulse duration leads to a reduction of the LIV pulse ramp A , and this yields a decrease of the BELIV current signal, if a LIV voltage range is kept invariable [13]. The decrease of the BELIV signal with enhancement of LIV pulse duration, due to reduction of LIV pulse ramp A , can be compensated by the increase of LIV voltage. C-DLTS is insufficiently sensitive to shallow traps with short thermal emission lifetime, when the injection pulse durations in the range of tens of microseconds are routinely used in DLT spectrometers. Thereby, combining of these C-DLTS and BELIV techniques can be efficient tool for examination of the large conductivity and capacitance samples.

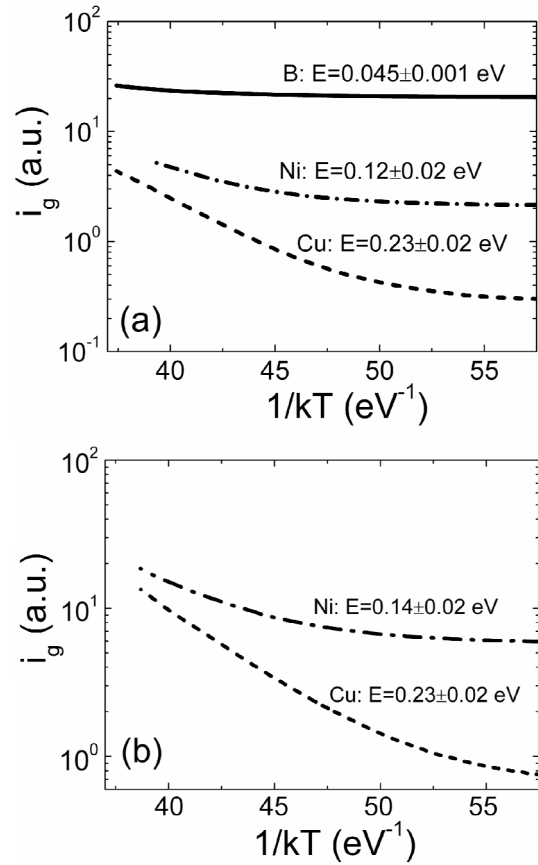


Fig. 3. Generation current (a) extracted from the BELIV transients recorded at 26 μ s (top curve), 260 μ s (middle curve) and 2.6 ms (bottom curve) LIV pulse duration, respectively, on solar cell fragment containing Ni/Cu electrodes. Generation currents (b) measured on solar cell fragment containing the Au top electrode with LIV pulse durations of 25 μ s (top curve) and 260 μ s (bottom curve), respectively

The BELIV transients have been recorded by varying durations of LIV pulses in the range from 2.6 μ s to 2.6 ms. The generation current component is extracted from the BELIV transients, therefore its dependence on temperature is examined. The different levels are temperature scanned for the different fixed LIV pulse durations: the shallower the examined level is, the shorter LIV pulse should be employed. Thereby, several temperature scan curves are obtained by varying the LIV pulse duration. These curves

then show different activation energy values, denoted in Figs. 3, a and b. The activation energy is represented by a slope of generation current plotted in the semilog scale as a function of the reverse thermal energy kT .

The traps with activation energy values of $E_B = (0.045 \pm 0.001)$ eV, $E_{Ni} = (0.12 \pm 0.02)$ eV and $E_{Cu-2} = (0.23 \pm 0.02)$ eV have been resolved in solar cell fragments containing Ni/Cu electrodes. These traps can be assigned to B dopants with $E_B = (0.045 \pm 0.001)$ eV, and to the nickel impurities with $E_{Ni} = (0.12 \pm 0.02)$ eV. The trap with activation energy of $E_{Cu-2} = (0.23 \pm 0.02)$ eV can be ascribed to copper impurities. This latter activation energy value might also be inherent to Ni, as referenced in literature [12], however, the value of the capture cross-section, attributed to Cu, is considerably larger. Therefore, the trap with activation energy of $E_{Cu-2} = (0.23 \pm 0.02)$ eV is assigned to the copper impurities in this consideration.

In samples made of solar cell fragment containing Au top electrode, the Ni ascribed traps with $E_{Ni} = (0.12 \pm 0.02)$ eV and the Cu attributed ones with activation energy of $E_{Cu-2} = (0.23 \pm 0.02)$ eV have been resolved, as well. This indicates, that Ni and Cu impurities were incorporated during the primary formation of electrodes on solar cells. The Cu impurities seem to form several deep levels with thermal activation energy values of $E_{Cu-2} = (0.23 \pm 0.02)$ eV, as determined from BELIV and C-DLTS temperature scans, and $E_{Cu-1} = (0.41 \pm 0.02)$ eV, as extracted from C-DLTS spectroscopy data.

4. CONCLUSIONS

The problem of usage of the standard deep level trap spectroscopy techniques appears in precise control of the introduced defects due to high conductivity base region in modern solar cells. This requires the extremely small area samples for the application of the standard C-DLTS instruments. The enhanced leakage current on sample boundaries is also inevitable for the small area solar cell fragments. Therefore, it is important to develop the alternative methods for the defect spectroscopy in the high conductivity junction structures. Therefore, the combined study of the dominant carrier killers has been performed in the as-fabricated industrial solar cells by using the capacitance deep level transient spectroscopy and the generation current temperature scan techniques. The technique of the barrier capacitance charging transients is beneficial as it enables ones to separate in time the barrier charging and generation current components. Signals of the barrier capacitance charging are even increased when the enhanced area samples are examined. The metal impurities of nickel introduce carrier traps with activation energy of $E_{Ni} = (0.12 \pm 0.02)$ eV, while copper impurities are responsible for the deep traps of activation energy values of $E_{Cu-2} = (0.23 \pm 0.02)$ eV and $E_{Cu-1} = (0.41 \pm 0.02)$ eV. Appearance of the traps with the same activation energy values, irrespective to the top metal layer, indicates that Ni and Cu impurities were incorporated during the primary

technological procedure in formation of electrodes on solar cells.

Acknowledgments

This study was partially supported by Lithuanian Science Council grant MIP-060/2013.

REFERENCES

1. **Sze, S. M., Ng, K. K.** Physics of Semiconductor Devices. John Wiley and Sons, Inc.. Hoboken, New Jersey, 2007.
2. **Gaubas, E.** Transient Absorption Techniques for Investigation of Recombination Properties in Semiconductor Materials *Lithuanian Journal Physics* 43 2003: pp. 145–165.
3. **Kaniava, A., Rotondaro, A. L. P., Vanhellemont, J., Menczgar, U., Gaubas, E.** Recombination Activity of Iron-related Complexes in Silicon Studied by Temperature Dependent Carrier Lifetime Measurements *Applied Physics Letters* 67 (26) 1995: pp. 3930–3932.
4. **You, J. S., Kang, J., Kim, D., Pak, J. J., Kang, C. S.** Copper Metallization for Crystalline Si Solar Cells *Solar Energy Materials and Solar Cells* 79 (3) 2003: pp. 339–345.
[http://dx.doi.org/10.1016/S0927-0248\(02\)00470-1](http://dx.doi.org/10.1016/S0927-0248(02)00470-1)
5. **Chow, K. M., Ng, W. Y., Yeung, L. K.** Barrier Properties of Ni, Pd and Pd-Fe for Cu Diffusion *Surface and Coating Technology* 105 (1–2) 1998: pp. 56–64.
6. **Leu, L. C., Norton, D. P., McElwee-White, L., Anderson, T. J.** Ir/TaN as a Bilayer Diffusion Barrier for Advanced Cu Interconnects *Applied Physics Letters* 92 (11) 2008: pp. 111917–111917-3.
7. **Blood, P., Orton, J. W.** The Electrical Characterization of Semiconductors: Majority Carriers and Electron States. Academic Press Inc., San Diego, 1992.
8. **Lang, D. V.** Deep-level Transient Spectroscopy: a New Method to Characterize Traps in Semiconductors *Journal of Applied Physics* 45 (7) 1974: pp. 3023–3032.
9. **Gaubas, E., Ceponis, T., Kusakovskij, J.** Profiling of Barrier Capacitance and Spreading Resistance by Transient Linearly Increasing Voltage Technique *Review of Scientific Instruments* 82 (8) 2011: pp. 083304–083304-4.
10. **Gaubas, E., Ceponis, T., Uleckas, A., Grigonis, R.** Room Temperature Spectroscopy of Deep Levels in Junction Structures Using Barrier Capacitance Charging Current Transients *Journal of Instrumentation* 7 2012: 01003 pp. 1–9.
11. **Gaubas, E., Čeponis, T., Sakalauskas, S., Uleckas, A., Velička, A.** Fluence Dependent Variations of Barrier and Generation Currents in Neutron and Proton Irradiated Si Particle Detectors *Lithuanian Journal Physics* 51 (3) 2011: pp. 230–236.
12. **Schroder, D. K.** Semiconductor Material and Device Characterization. 3rd Ed. John Wiley and Sons, New Jersey, 2006.
13. **Gaubas, E., Ceponis, T., Vaitkus, J.** Impact of Generation Current on the Evaluation of the Depletion Width in Heavily Irradiated Si Detectors *Journal of Applied Physics* 110 2011: pp. 033719–033719-7.